

Supplementary Information

for

Nitrogen-Doped Graphene Networks Supported Copper Nanoparticles Encapsulated with Graphene Shells for Surface-Enhanced Raman Scattering

Xiang Zhang^a, Chunsheng Shi^a, Enzuo Liu^{a, b}, Jiajun Li^a, Naiqin Zhao^{*, a, b} and
Chunnian He^{*, a, b}

^a *School of Materials Science and Engineering and Tianjin Key Laboratory of
Composites and Functional Materials, Tianjin University, Tianjin, 300072, P. R.
China*

^b *Collaborative Innovation Center of Chemical Science and Engineering, Tianjin
300072, China*

* Address correspondence to

cnhe08@tju.edu.cn, nqzhao@tju.edu.cn

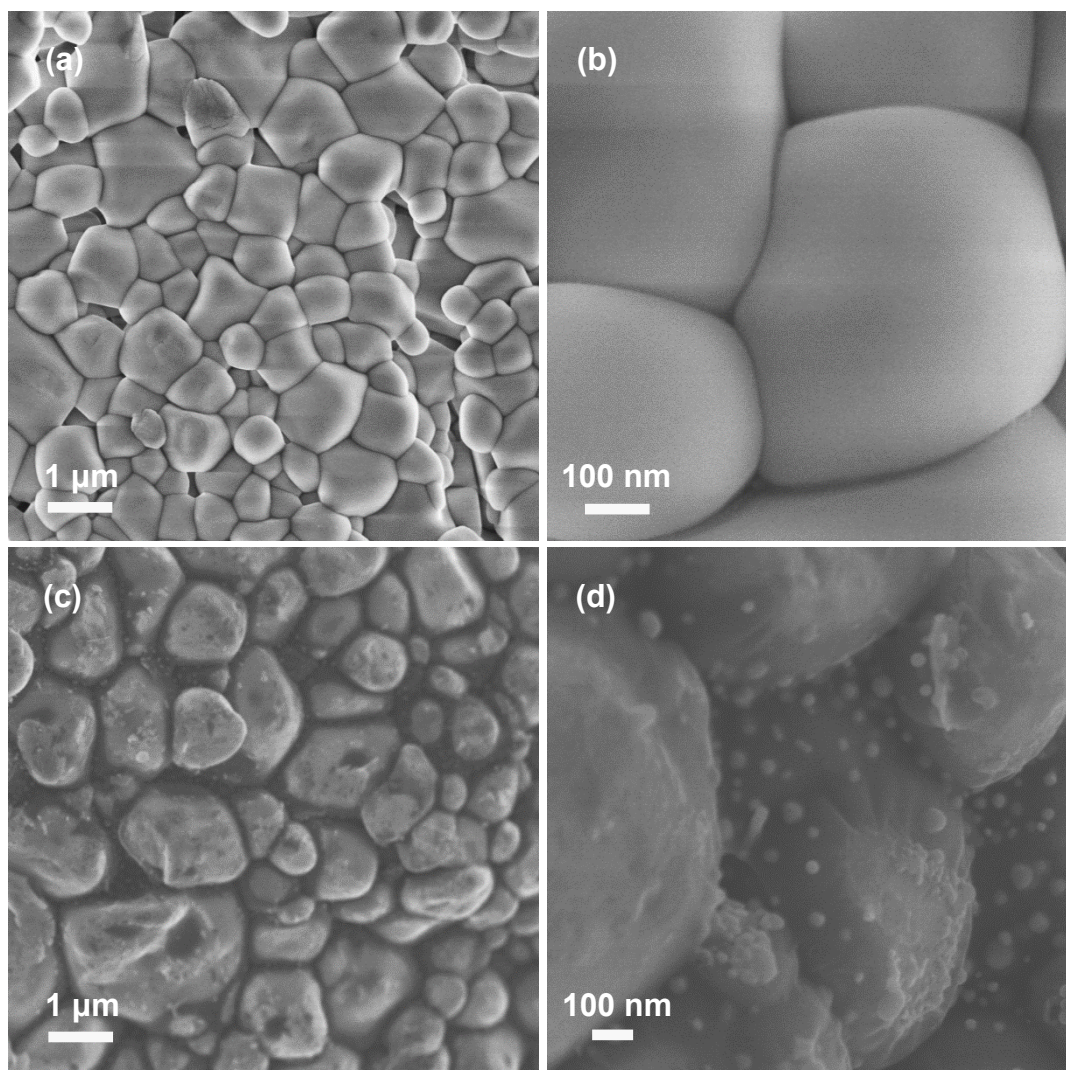


Fig. S1. a) and b) SEM images of the precursor powder of $\text{Cu}(\text{NO}_3)_2\text{-C}_6\text{H}_{12}\text{O}_6/\text{CO}(\text{NH}_2)_2\text{-NaCl}$ after freeze-drying, suggesting that the NaCl particles uniformly coated with a thin film of $\text{Cu}(\text{NO}_3)_2\text{-C}_6\text{H}_{12}\text{O}_6/\text{CO}(\text{NH}_2)_2$ complex were self-assembled to 3D structure during the freeze-drying process. c) and d) SEM images of the CVD-synthesized Cu@G-NGNs products before eliminating the NaCl, showing that the 3D self-assembly was well preserved after CVD process and the Cu@G-NGNs were formed on the surface of 3D NaCl self-assembly.

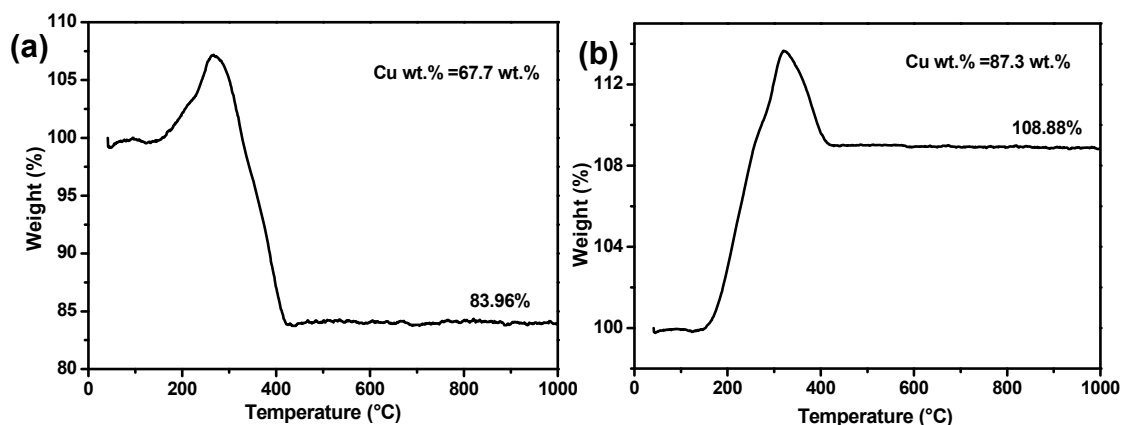


Fig. S2. Thermogravimetric analysis of (a) Cu-50 and (b) Cu-240 in air condition. By the same calculation method described in the text, the weight percentage of Cu for Cu-50 and Cu-240 were calculated as 67.7 wt.% and 87.3 wt.%, respectively.

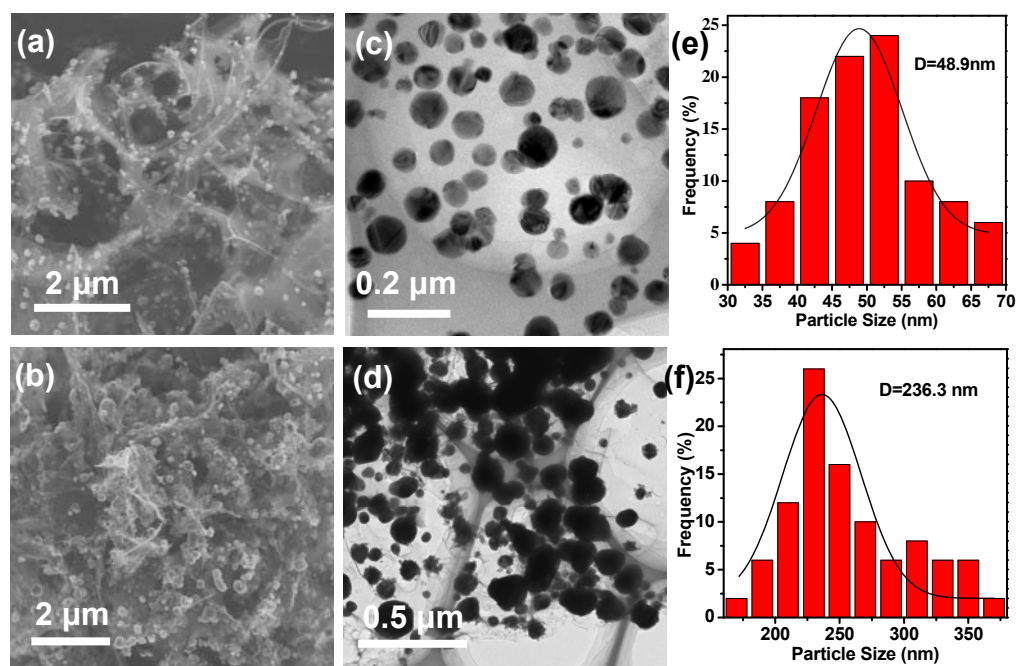


Fig. S3. SEM images of the resulting materials' morphology: (a) Cu-50 and (b) Cu-240. TEM images of (c) Cu-50 and (d) Cu-240. (e-f) The corresponding particle size distribution of Fig. S3(c) and (d), respectively (Each calculated from 50 NPs). The average size calculated for the two samples were 48.9 nm (~50 nm) and 236.3 nm (~240 nm).

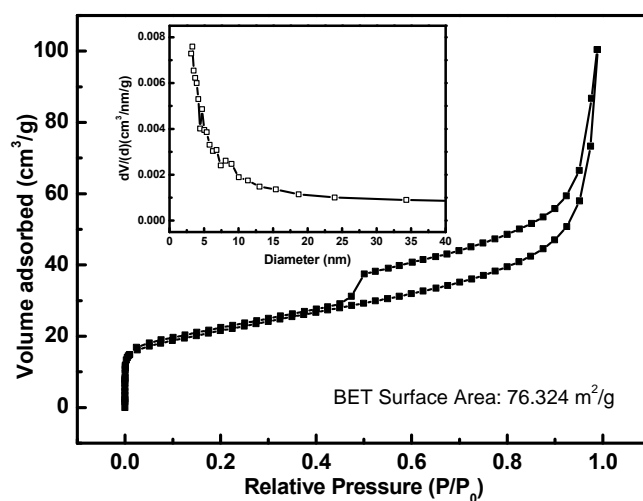


Fig. S4. Nitrogen adsorption–desorption isotherms, and inset is pore size distribution curve of Cu@G-NGNs.

Table S1. Detailed information of comparison of the BET specific surface area between Cu@G-NGNs and reported metallic SERS substrate as well as rGO/Cu NPs composites.

Sample Name	BET Specific Surface Area (m ² /g)	Metal wt. %	References
Cu@G-NGNs	76.324	79.3%	This work
Cu butterfly wings	56.6	100%	S1
Ag sponges	39	100%	S2
Ag hollow spheres	30.9	100%	S3
Au–Pd foams	20.19	100%	S4
rGO/Cu NPs	29.96	>63%	S5

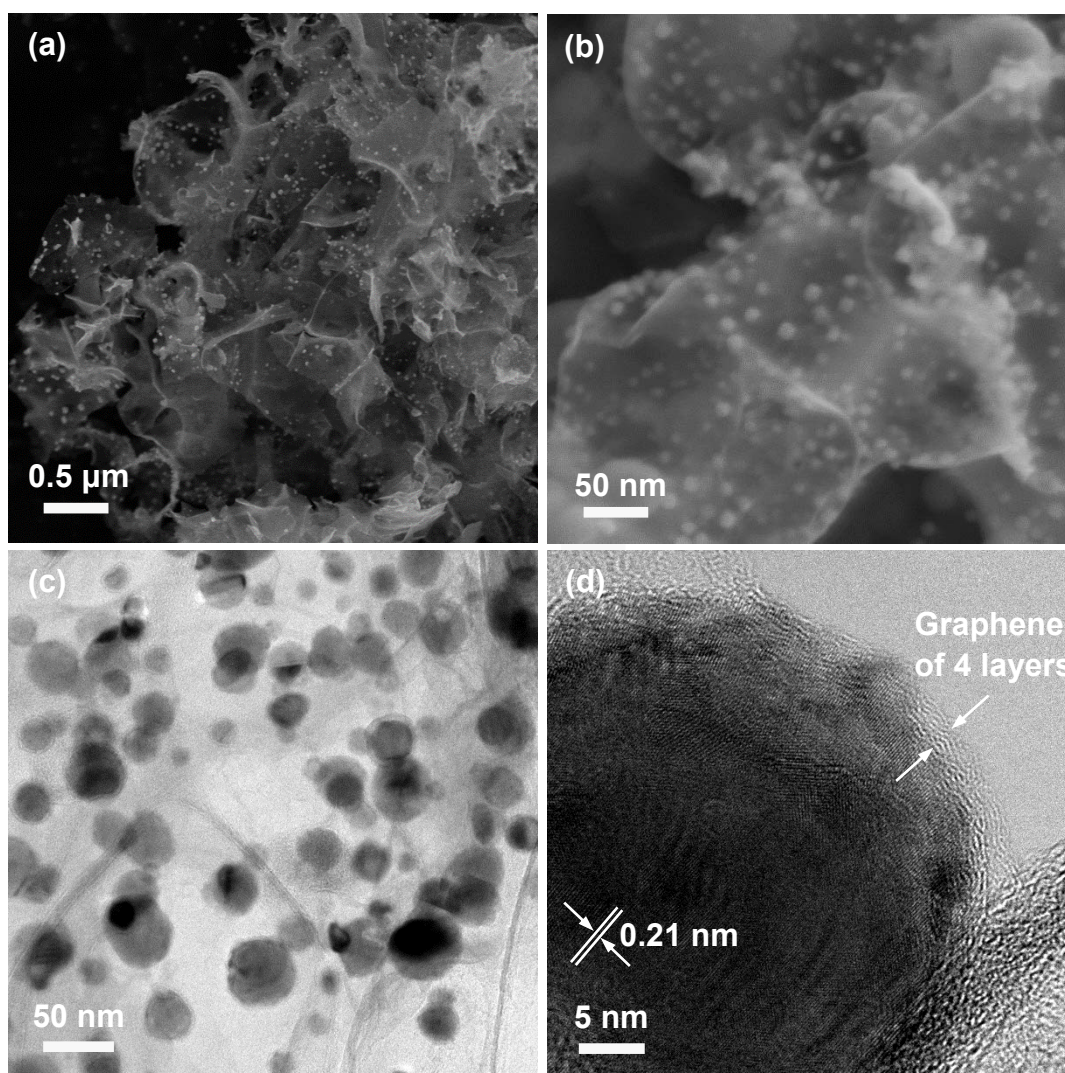


Fig. S5. a) and b) SEM, c) and d) HRTEM images of the Cu@G-GNs, showing a similar morphology with Cu@G-NGNs. The graphene walls were homogenously decorated with Cu NPs (5-30 nm).

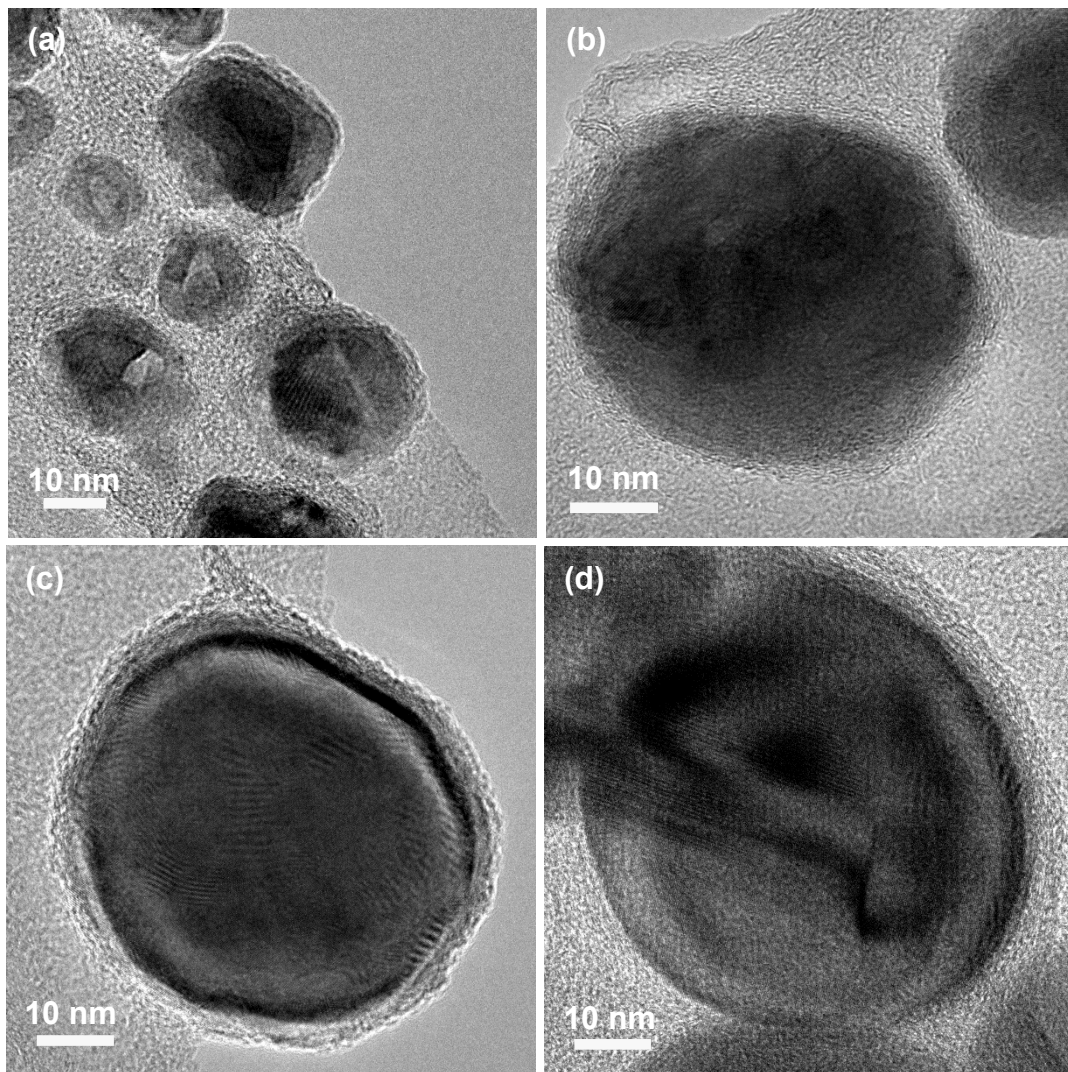


Fig. S6. HRTEM images of Cu@G nanoparticles, showing that Cu nanoparticle is entirely encapsulated by thin graphene shells (~ 1 nm) tightly anchored on the graphene walls from the 3D network.

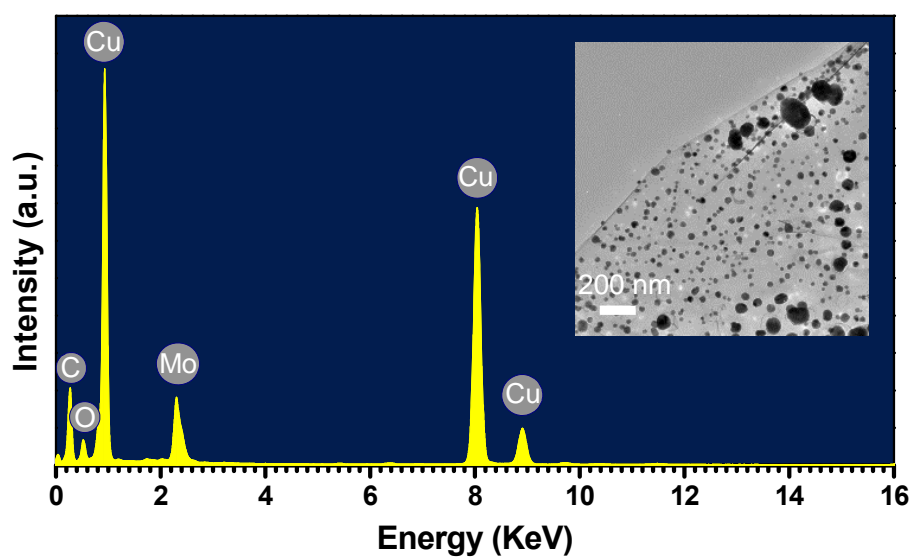


Fig. S7. EDS pattern and corresponding TEM image (inset) of Cu@G-NGNs.

The EDS sample was prepared using Cu@G-NGNs powder dispersed in ethanol followed by short-time ultrasonification. A small drop of this dispersion was placed on a carbon coated Mo grid, dried under ambient conditions.

Table S2. The detailed element contents of EDS analysis in Fig. S7.

Element	Weight Ratio (%)	Atomic Ratio (%)
C K	16.23	47.48
O K	3.77	8.28
Cu K	80.00	44.23

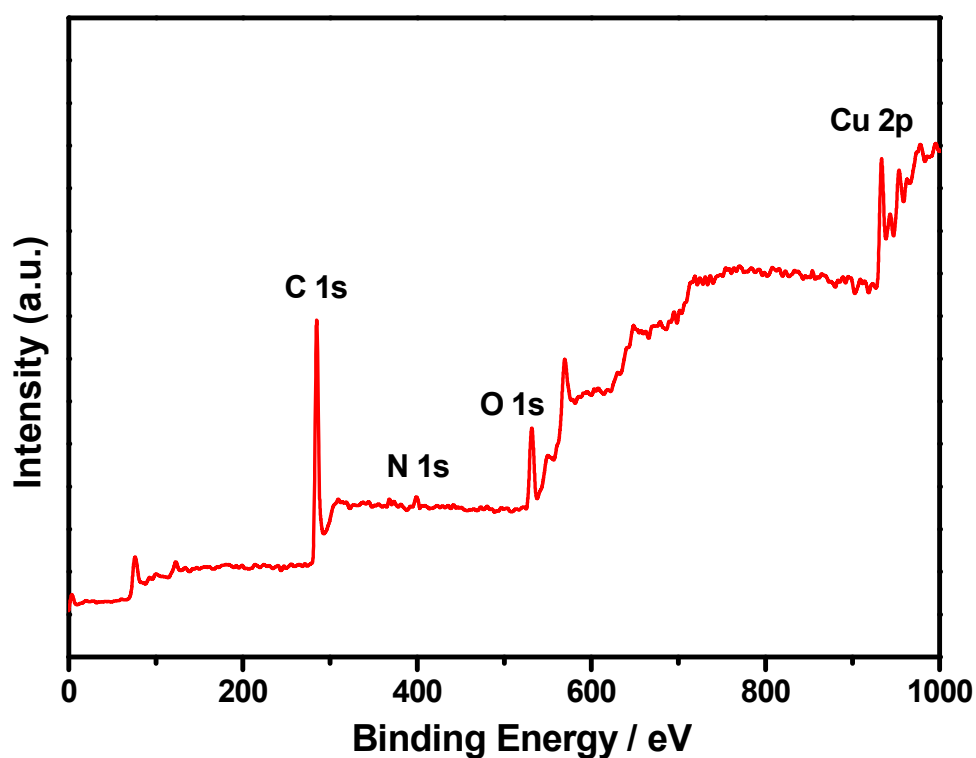


Fig. S8. The XPS full spectrum of Cu@G-NGNs.

Table S3. The relative element ratio of XPS analysis in Fig.S8.

Element	C1s	N1s	O1s	Cu2p3
Relative Atomic Ratio (%)	81.97	0.92	13.41	3.7
Binding Energy (eV)	284.32 288.58	399.42	529.61 531.91	932.35

The relative content of N element (At%) doped in graphene was calculated by the following equation:

$$At\% = \frac{A_{N1s}}{A_{C1s} + A_{N1s}} \times 100\% = 0.92 / (81.97 + 0.92) * 100\% = 1.10\%.$$

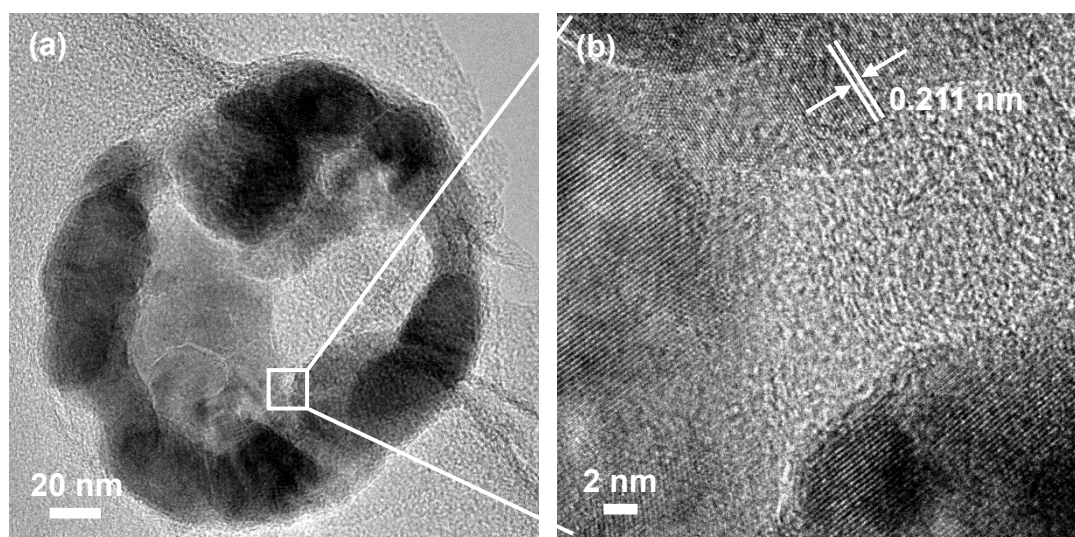


Fig. S9. HRTEM images of the aggregation and interdiffusion of the Cu_n/C nanoclusters. b) is the magnified TEM image of the selected area in a).

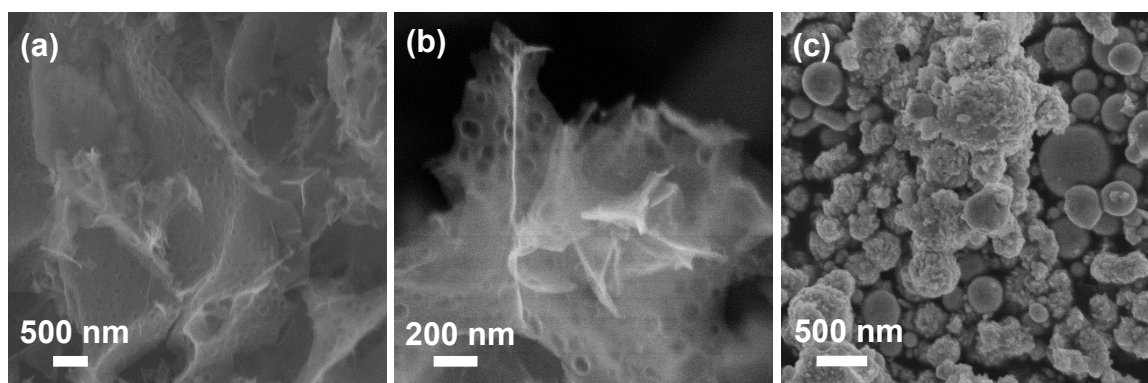


Fig. S10. a) and b) SEM images of NGNs obtained by etching Cu NPs from the $\text{Cu}@G\text{-NGNs}$ composites. c) SEM images of commercial Cu NPs with average size of 50 nm.

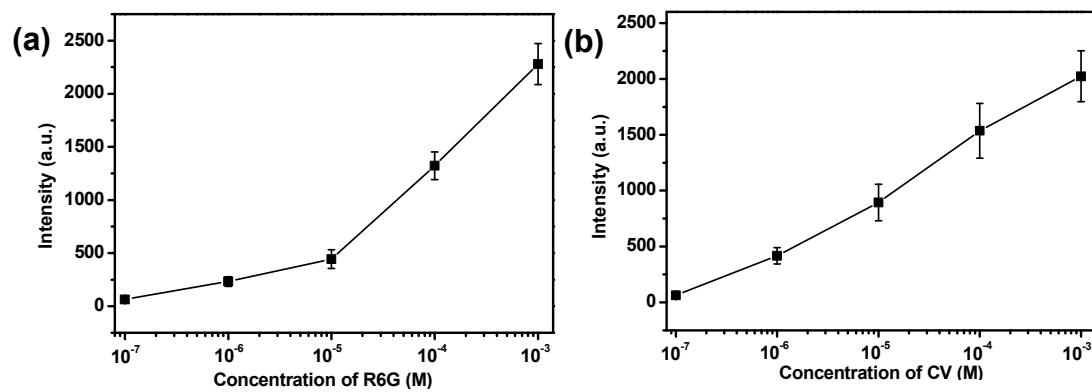


Fig. S11. (a) The intensity of SERS signal versus the concentration of (a) R6G at 612 cm^{-1} , and (b) CV at 1170 cm^{-1} for Cu@G-NGNs (Cu-20) substrate. 5 spectra of different spots were used to calculate the intensity for each concentration.

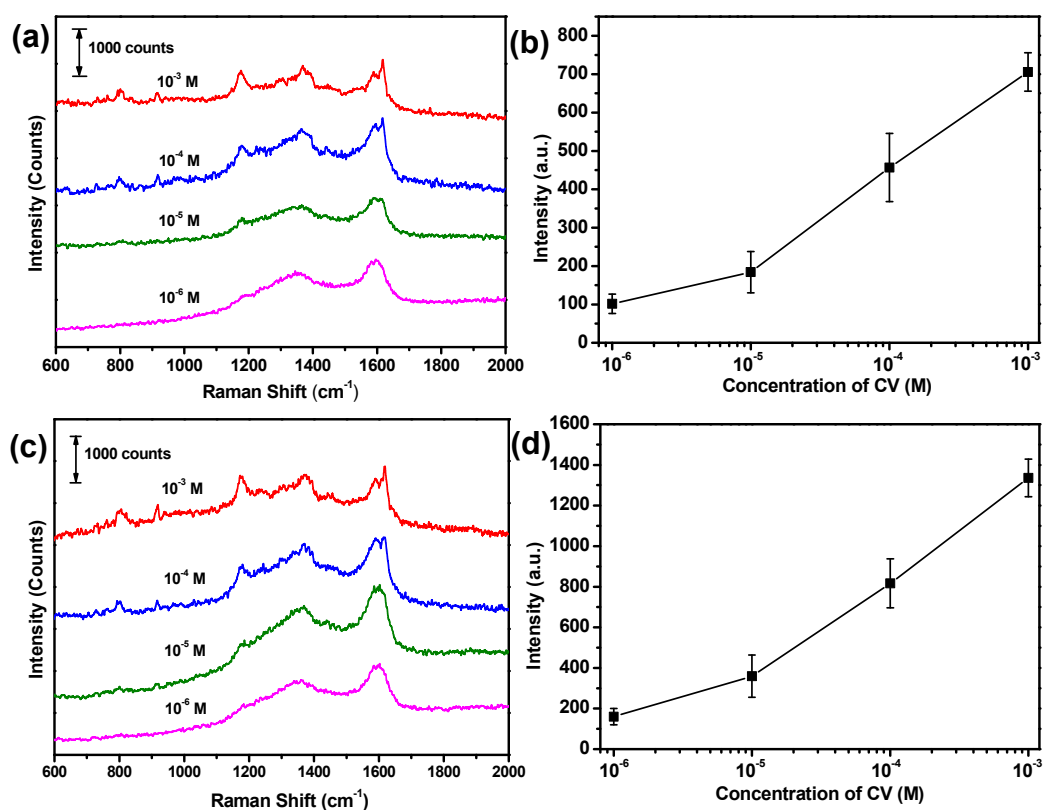


Fig. S12. SERS spectra of CV at different concentrations adsorbed on (a) Cu-50 and (c) Cu-240 substrate. The corresponding intensity of SERS signal versus the concentration of CV at 1170 cm^{-1} for (b) Cu-50 and (d) Cu-240 substrate, respectively. 5 spectra of different spots were used to calculate the intensity for each concentration.

Detailed calculation of enhancement factor

The SERS enhancement factors (EF) for R6G can be calculated according to the equation

$$EF = \frac{I_{SERS} \times N_{bulk}}{I_{bulk} \times N_{SERS}}$$

Where I_{SERS} and I_{bulk} are the integrated intensities of R6G molecules adsorbed on the Cu@G-NGNs substrate and from 10^{-2} M of R6G bulk solution, respectively. N_{SERS} and N_{bulk} are the corresponding numbers of R6G molecules adsorbed on the Cu@G-NGNs substrate and in the bulk solution in the focal volume of the laser beam, respectively.

For valuable determination of N_{bulk} and N_{SERS} , 5 μ L R6G solution of 10^{-2} M and 10^{-5} M were carefully dropped on glass and Cu@G-NGNs substrates, respectively.

$$N_{bulk} = Ahc_{bulk} N_A$$

Where A is the area of the laser focal spot (diameter of 1 μ m), h is the confocal depth of the laser (15 μ m), which is calculated by a modified equation in a similar

method:^{S6}
$$h = \int_0^{\infty} I(z) dz / I_0$$

Where $I(z)$ is the intensity of the Raman peak of glass (1093 cm^{-1}), which is measured as a reference to calculate h . Considering the transparent feature of glass substrate, it is meaningless to calculate the intensity below the focal plane of glass substrate in Fig. S13. So the measured h is an underestimated result.

c_{bulk} is the concentration of R6G bulk solution, here $c_{bulk} = 10^{-2}$ M, and N_A is the Avogadro constant.

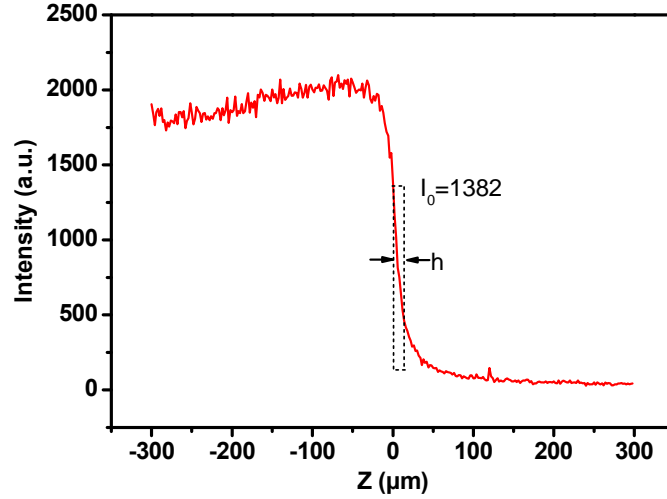


Fig. S13. Raman intensity-depth profile of the intensity of 1093 cm^{-1} band for a glass slide substrate.

Provided that R6G molecules were in monolayer adsorption on the Cu@G-NGNs SERS substrate:

$$N_{SERS} = \frac{c_{SERS} \nu N_A A}{\pi r^2}$$

$$N_{bulk} / N_{SERS} = \frac{\pi r^2 h c_{bulk}}{\nu c_{SERS}} = [3.14 \times (4.0 \times 10^{-3})^2 \times (15 \times 10^{-6}) \times (1 \times 10^{-2})] / [(5 \times 10^{-9}) \times (1.0 \times 10^{-5})] =$$

150.72

Where c_{SERS} is the concentration of R6G solution for SERS, $c_{SERS} = 10^{-5}\text{ M}$, $\nu = 5\text{ }\mu\text{L}$, r is the radius of $5\text{ }\mu\text{L}$ R6G solution formed on the SERS substrate, $r = 4.0\text{ mm}$.

Fig. S14 (a) and (b) are the normal Raman spectrum of 10^{-2} M of R6G solution and SERS spectrum of 10^{-5} M of R6G solution acquired from the Cu@G-NGNs substrate. The integrated intensities of the bands for I_{bulk} (612 cm^{-1}) and I_{SERS} (610 cm^{-1}) were 1067 and 8122 cps, respectively. Considering the different number of molecules in each unit volume for normal Raman spectrum on glass substrate and SERS spectrum on the Cu@G-NGNs substrate,^{S7} $I_{SERS} / I_{bulk} = 8122 \times 10^3 / 1067$.

Finally, the EF of the Cu@G-NGNs substrate was calculated as 1.15×10^6 , which is an underestimated result.

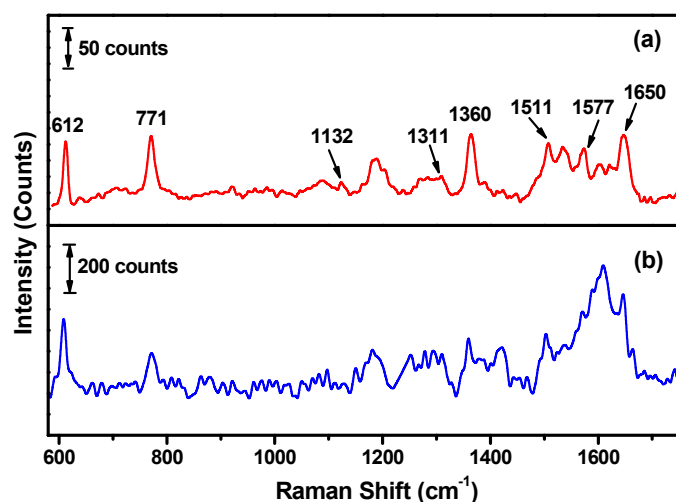


Fig. S14. (a) Normal Raman spectrum of 10^{-2} M R6G solution. Laser power: 0.5 mW. (b) SERS spectrum of 10^{-5} M R6G solution acquired from the Cu@G-NGNs substrate. Laser power: 0.5 mW. Baselines of both spectra were removed for the comparison.

References:

- S1 Y. Tan, J. Gu, W. Xu, Z. Chen, D. Liu, Q. Liu, D. Zhang, *ACS Appl. Mater. & Interf.*, 2013, **5**, 9878-9882.
- S2 S. Tang, S. Vongehr, Y. Wang, J. Cui, X. Wang, X. Meng, *J. Mater. Chem. A*, 2014, **2**, 3648-3660.
- S3 Y. Wang, T. Gao, K. Wang, X. Wu, X. Shi, Y. Liu, S. Lou, S. Zhou, *Nanoscale*, 2012, **4**, 7121-7126.
- S4 H. Liu, Q. Yang, *J. Mater. Chem.*, 2011, **21**, 11961-11967.
- S5 A. Ehsani, B. Jaleh, M. Nasrollahzadeh, *J. Power Sources*, 2014, **257**, 300-307.
- S6 W. Cai, B. ren, X. Li, C. She, F. Liu, X. Cai, Z. Tian, *Surf. Sci.*, 1998, **406**, 9-22.
- S7 J. Chen, B. Shen, G. Qin, X. Hu, L. Qian, Z. Wang, S. Li, Y. Ren, L. Zuo, *J. Phys. Chem. C*, 2012, **116**, 3320-3328.